PERGAMON

International Journal of Solids and Structures 36 (1999) 1677–1699

INTERNATIONAL JOURNAL OF SOLIDS and STRUCTURES

Methods of interconversion between linear viscoelastic material functions. Part II—an approximate analytical method

R. A. Schapery[a,*], S. W. Park[b]

[a] *Department of Aerospace Engineering and Engineering Mechanics, The University of Texas at Austin, Austin TX 78712, U.S.A.*

[b] *School of Mechanical Engineering, Georgia Institute of Technology, Atlanta GA 30332, U.S.A.*

Received 31 July 1997; in revised form 17 February 1998

Abstract

A new, very simple approximate interconversion method is proposed and verified by examples. This technique, employing the slope of the source function on logarithmic scales, is found to substantially enhance the accuracy compared to existing approximate methods. The new method is based on the characteristic mathematical properties of the narrow-band weight functions involved in the interrelationships between broad-band material functions. With the material functions represented locally by a power law, they are interrelated in terms of adjustment factors expressed through the local, log–log slope of the given (source) function. A number of existing approximate interconversion methods are also tested and compared with the new method. In Part I (Park and Schapery, 1998), an efficient numerical interconversion method, based on a Prony (exponential) series representation of both the source and target functions, was presented; such a series representation is not needed here. The new method, when applied to the prediction of broad-band time-dependent functions from Laplace or Fourier transforms, is an approximate method of transform inversion that is applicable to functions which are not necessarily viscoelastic material functions.

Keywords: Viscoelasticity; Interconversion; Material functions; Power-law representation; Transform inversion

1. Introduction

There are many times that one wants to predict one viscoelastic material function from another or to invert a Laplace or Fourier transform in a variety of problems. For example, it may be of interest to determine a transient material function, like relaxation modulus or creep compliance at very small times. It is often experimentally advantageous to get this from the corresponding

* Corresponding author. Fax: 001 (512) 471-5500; e-mail: schapery@uts.cc.utexas.edu

0020–7683/99/$ - see front matter
PII: S0020–7683(98)00060–2

complex material function in the frequency domain (obtained through a test with a steady-state sinusoidal input) rather than determining the transient function directly from a short-time relaxation or creep test. In some applications one may need the creep compliance when only the relaxation modulus is available or vice versa. Analysis of a viscoelastic continuum using the elastic-viscoelastic correspondence principle is based on the use of Laplace or Fourier transforms of related material functions to derive transformed response functions, which then requires transform inversion to predict time-dependent response.

In Part I (Park and Schapery, 1998), we presented and tested a numerical method of interconversion between modulus and compliance functions when the given (source) and predicted (target) functions are based on a Prony (exponential) series representation of transient functions. It was shown that the determination of a target function simply reduced to solving a system of linear algebraic equations for unknown Prony series coefficients, without the need to derive the target time constants. For ease of reference later in this paper, expressions in terms of Prony series constants for time and frequency dependent moduli are summarized in Appendix A.

In this paper we concentrate on approximate analytical interrelationships. It should be emphasized that, although the material characterization used here in the examples starts with a Prony series, such a representation is not needed. Indeed, it would be sufficient to start with numerical values of modulus or compliance obtained directly from an experiment; some smoothing of the data may be needed because the slope in logarithmic coordinates is required.

Some existing methods are reviewed first. Then the narrow band property of the weight functions involved in various interrelationships between the material function is discussed. Based on these properties and the broad band representation of actual material functions, a set of new, easily applied, approximate analytical interconversions are developed and illustrated using a set of experimental data from polymethyl methacrylate (PMMA). The new models are compared with existing models in their simplicity, accuracy, and limitations.

2. Some existing approximate interconversion methods

A large number of approximate, analytical interconversion methods with different bases and accuracies have been proposed by others (e.g., see Tschoegl, 1989). Among these, a few methods will be selected and discussed, and then their performances compared with our new method.

Schapery (1962) presented two approximate methods of Laplace transform inversion, the direct method and the collocation method. As a special application of the direct method, the uniaxial relaxation modulus $E(t)$ and the operational modulus (defined as the Carson transform or the s-multiplied Laplace transform of the relaxation modulus),

$$\tilde{E}(s) \equiv s\int_0^\infty E(t)\,e^{-st}\,\mathrm{d}t = s\int_{-\infty}^\infty E(t)t\,e^{-st}\,\mathrm{d}(\ln t) \tag{1}$$

have the following approximate interconversion properties:

$$E(t) \cong \tilde{E}(s)|_{s=(\alpha/t)} \quad \text{or} \quad \tilde{E}(s) \cong E(t)|_{t=(\alpha/s)} \tag{2}$$

where $\tilde{E}(s) \equiv s\bar{E}(s)$ and $\bar{E}(s)$ is the Laplace transform of the function $E(t)$; throughout this paper

$\ln(\cdot)$ and $\log(\cdot)$ denote the logarithms using base e and base 10, respectively. Also, $\alpha = e^{-C}$ where $C = 0.5772\ldots$ is Euler's constant, resulting in $\alpha \cong 0.56$.

The relationship (2) yields good results whenever the derivative of $E(t)$ with respect to $\log t$ is a slowly varying function of $\log t$. Schapery (1962) also proposed an improved relationship for the case in which the derivative of $\log E(t)$ with respect to $\log t$ is a slowly varying function of $\log t$,

$$E(t) \cong \tilde{E}(s)|_{s=(\beta/t)} \quad \text{or} \quad \tilde{E}(s) \cong E(t)|_{t=(\beta/s)} \tag{3}$$

where $\beta = \{\Gamma(1-n)\}^{-(1/n)}$. Also $\Gamma(\cdot)$ denotes the Gamma function and n is the local log–log slope of the source function defined by either $n \equiv -\mathrm{d}\log E/\mathrm{d}\log t$ or $n \equiv \mathrm{d}\log \tilde{E}/\mathrm{d}\log s$. It is easily shown, by using (1), that (3) is exact for all $t > 0$ if $E(t) \sim t^{-n}$ and n is constant. When the moduli in (2) and (3) are replaced by compliances, denoted by D's, one may obtain analogous relationships between the creep compliance $D(t)$ and the operational compliance $\tilde{D}(s)$.

Christensen (1982) proposed an approximate interconversion between the relaxation modulus and the storage modulus $E'(\omega)$ of the following form:

$$E(t) \cong E'(\omega)|_{\omega=(2/\pi t)} \quad \text{or} \quad E'(\omega) \cong E(t)|_{t=(2/\pi\omega)} \tag{4}$$

A similar relationship holds for compliance functions when E's in (4) are replaced by D's.

Staverman and Schwarzl (1955) gave the following approximate conversion from $E'(\omega)$ to the loss modulus $E''(\omega)$:

$$E''(\omega) \cong \frac{\pi}{2}\frac{\mathrm{d}E'(\omega)}{\mathrm{d}\ln\omega} \tag{5}$$

The relation (5) was later modified by Schwarzl and Struik (1967) by including an additional higher-order term which requires a triple derivative of $E'(\omega)$ with respect to $\mathrm{d}\ln\omega$.

Finally, Booij and Thoone (1982) proposed the following conversion from $E''(\omega)$ to $E'(\omega)$:

$$E'(\omega) \cong E_\mathrm{e} - \frac{\pi\omega}{2}\frac{\mathrm{d}[E''(\omega)/\omega]}{\mathrm{d}\ln\omega} \tag{6}$$

which may be rewritten as

$$E'(\omega) \cong E_\mathrm{e} + \frac{\pi}{2}\left(1 - \frac{\mathrm{d}\ln E''}{\mathrm{d}\ln\omega}\right)E''(\omega) \tag{7}$$

where E_e is the equilibrium (or rubbery) modulus. Relations (5)–(7) also apply to compliances when E' and E'' are replaced by D' and $-D''$, respectively.

3. Motivation and theoretical basis for the new method

Many of the approximate interconversion methods are based on different kinds of simplifications made in their original exact mathematical interrelationships. These simplifications are associated with the unique nature of the weight function involved in each interrelationship. From the theory of viscoelasticity, the following exact relations between two material functions may be obtained (e.g., Tschoegl, 1989):

$$E(t) = \frac{2}{\pi}\int_0^\infty E'(\omega)\frac{\sin\omega t}{\omega}\,\mathrm{d}\omega \tag{8}$$

$$E(t) = E_\mathrm{e} + \frac{2}{\pi}\int_0^\infty E''(\omega)\frac{\cos\omega t}{\omega}\,\mathrm{d}\omega \tag{9}$$

$$E'(\omega) = E_\mathrm{e} + \frac{2\omega^2}{\pi}\int_0^\infty E''(\lambda)\frac{1}{\lambda(\omega^2-\lambda^2)}\,\mathrm{d}\lambda \tag{10}$$

$$E''(\omega) = \frac{2\omega}{\pi}\int_0^\infty [E'(\lambda)-E_\mathrm{e}]\frac{1}{\lambda^2-\omega^2}\,\mathrm{d}\lambda \tag{11}$$

Equations (10) and (11) are known as Kronig–Kramers relations; the integrals are to be interpreted as Cauchy principal values. The Carson transforms of (8) and (9) are,

$$\tilde{E}(s) = \frac{2s}{\pi}\int_0^\infty E'(\omega)\frac{1}{s^2+\omega^2}\,\mathrm{d}\omega \tag{12}$$

$$\tilde{E}(s) = E_\mathrm{e} + \frac{2s^2}{\pi}\int_0^\infty E''(\omega)\frac{1}{\omega(s^2+\omega^2)}\,\mathrm{d}\omega \tag{13}$$

Interconversion methods (2) and (3) are based on the specific narrow band character of the factor $(st\,e^{-\mathrm{st}})$ involved in (1) when a logarithmic time scale is used in the integral. Specifically, Schapery (1962) discussed the relationship between a viscoelastic transient function $\psi(t)$ and its corresponding Carson transform $s\bar{\psi}$. He derived the following relationship between this transform and the transient function with logarithmic independent variables:

$$\hat{f}(u) = \int_{-\infty}^\infty g(w)f(w-u)\,\mathrm{d}w \tag{14}$$

where $\hat{f}(u) \equiv s\bar{\psi}(s)$, $f(v) \equiv \psi(t)$, $\bar{\psi}(s) \equiv \int_0^\infty \psi(t)\,\mathrm{e}^{-st}\,\mathrm{d}t$, $g(w) \equiv (\ln 10)\ 10^w \exp(-10^w)$, $u \equiv \log s$, $v \equiv \log t$, $w = u+v$, and, as noted earlier, $\log \equiv \log_{10}$. The weight function $g(w)$ is small outside of a roughly two-decade range $-1.25 \leqslant w \leqslant 0.75$ centered at the centroid $w_\mathrm{c} \equiv \log(e^{-C}) \cong -0.25$, as illustrated in Fig. 1. In other words, the value of a Carson transform at a particular s-value is dictated primarily by the variation of the corresponding transient function within the t-range of $-\log s-1 < \log(t/\alpha) < -\log s+1$, where $\alpha = e^{-C} \cong 0.56$. If the weight function is replaced by a Dirac delta function $\delta(w-w_\mathrm{c})$, an approximate inversion formula, $f(w_\mathrm{c}-u) \cong \hat{f}(u)$, is obtained; equivalently, $\psi(t) \cong s\bar{\psi}(s)|_{s=(\alpha/t)}$ in terms of the original functions. This result is easily shown to be exact when $s\bar{\psi}$ is linear in $\log s$ for all $s > 0$. In view of the narrow-band character of the weight function, the relationship will be a good approximation for a function $\psi(t)$ that can be approximated on a logarithmic time scale by piecewise straight lines that are two decades wide. An improved approximation that accounts for curvature was given later by Schapery (1974). Equation (3) follows from a similar argument if $\psi \sim t^n$ and n is a slowly varying function of $\log t$. Schapery (1962) also observed that integrals like that in (12) may be approximated in a similar fashion (if n

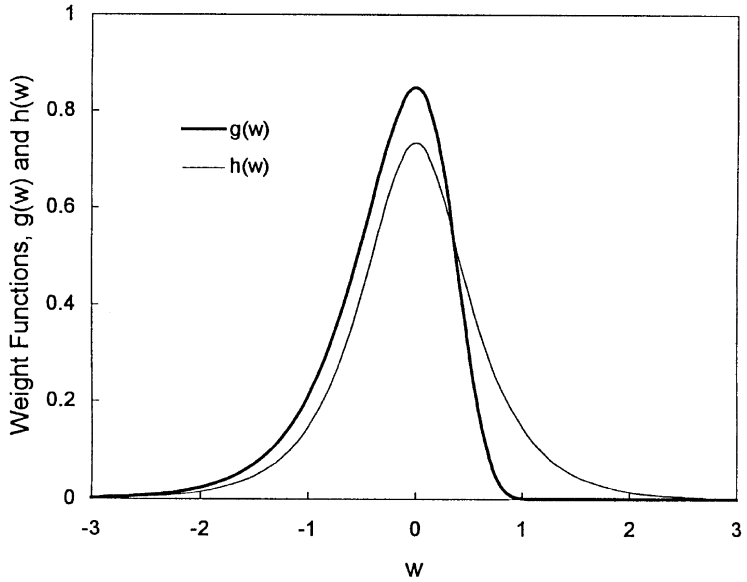

Fig. 1. The weight functions $g(w)$ and $h(w)$ used in (14) and (20).

is not close to -1) because they too can be expressed in terms of a narrow band weight function, designated by $h(w)$ in Fig. 1.

In deriving (4), Christensen (1982) used an approximation of the weight function, $(\sin \omega t)/\omega$, in (8) by replacing it with $(\pi/2)\delta(\omega-\omega_0)$ where $\delta(\cdot)$ is the Dirac delta function. The parameter w_0 was determined by assuming that $E'(\omega)$ is a linear function of ω in the neighborhood of ω_0, and $\omega_0 = 2/(\pi t)$ resulted. The definite integral $\int_0^\infty (\sin \eta/\eta)\, \mathrm{d}\eta = \pi/2$ was used to determine the normalizing factor $\pi/2$.

Here we shall expand on these ideas in developing some new approximations, placing emphasis on material functions of the power law type, t^n or ω^n, where n is a slowly varying function of $\log t$ or $\log \omega$ and is in the range of $-1 < n < 1$; this latter restriction assures convergence of the relevant integrals and covers almost all cases of practical interest.

First, let us write the relaxation modulus in the form

$$E(t) = E_n \left(\frac{t}{t_n}\right)^{-n} [1+F(t)] \tag{15}$$

where $E_n \equiv E(t_n)$. Note that $F \equiv 0$ for a pure power law representation. The function F accounts for an arbitrary departure from a power law; the time t_n is the time at which the negative of the slope, $n \equiv -\mathrm{d}\log E/\mathrm{d}\log t$, is evaluated. Considering the definition of E_n and n, it follows from (15) that

$$F(t_n) = \frac{\mathrm{d}F}{\mathrm{d}t}(t_n) = 0 \tag{16}$$

The Carson transform of (15) is

$$\tilde{E}(s) = E_n\Gamma(1-n)(st_n)^n[1+c_n] \tag{17}$$

where

$$c_n \equiv s^{1-n}\int_{-\infty}^{\infty} Ft^{1-n}\,e^{-st}\,\mathrm{d}(\ln t)/\Gamma(1-n) \tag{18}$$

is the relative correction due to the departure from a pure power law. If c_n is neglected (as motivated by the narrow band character of the weight function in Fig. 1), and we choose $t_n = 1/s$, then (17) may be written in the form,

$$\tilde{E}(s) = \Gamma(1-n)E(t) \quad \text{with} \quad t = 1/s \tag{19}$$

which is equivalent to (3) if n is constant. Both (3) and (19) produce essentially the same results when n varies slowly; here we choose to use form (19) because of its greater simplicity, especially when two conversion steps are used, as discussed below.

A better choice for t_n is a value that minimizes the correction c_n, given s. As shown in Appendix B, this choice depends on the value of n at the initially unknown time t_n. The value of $\log(st_n)$ for the optimum t_n is estimated to be only a fraction of a decade in most cases (i.e., when $n \leqslant 0.5$), and the result depends on the initially unknown value of n. Motivated by these facts, we shall use $\log(st_n) = 0$ as implied by (19), although it is recognized that an iterative process could be used to reduce the error in (19) through a better choice of t_n. In the example of PMMA given later, $n \leqslant 0.4$.

The Carson transform $\tilde{E}$ in terms of E' is given in (12). This integral may be approximated using arguments similar to those leading to (19). The counterpart to (14) is

$$\hat{f}(u) = \int_{-\infty}^{\infty} h(w)\,f(w+u)\,\mathrm{d}w \tag{20}$$

where $\hat{f}$ and u are as before; but here $f(v) \equiv E'(\omega)$, $v \equiv \log\omega$, $w \equiv v-u = \log(\omega/s)$, and the weight function $h(w)$ is

$$h(w) \equiv \frac{2}{\pi}\frac{\ln 10}{(10^{-w}+10^{w})} \tag{21}$$

This function is plotted in Fig. 1. As may be observed, it is symmetric with respect to $w = 0$, and is small outside a roughly two-decade range. Let us use a representation for E' which is analogous to that in (15),

$$E'(\omega) = E'_n\left(\frac{\omega}{\omega_n}\right)^n\left[1+F'\left(\frac{\omega}{\omega_n}\right)\right] \tag{22}$$

where $E'_n \equiv E'(\omega_n)$ and $n \equiv \mathrm{d}\log E'/\mathrm{d}\log\omega$. Neglecting the contribution of F' to the integral, together with selecting $\omega_n = s$, we find

$$\tilde{E}(s) = \frac{E'(\omega)}{\cos(n\pi/2)} \quad \text{with} \quad \omega = s \tag{23}$$

An improved choice of ω_n is given in Appendix B but, as before, it does not differ much from s on a logarithmic scale when $n \leqslant 0.5$.

Equations (19) and (23) may be used to eliminate $\tilde{E}$, so that

$$E'(\omega) = \Gamma(1-n)\cos\left(\frac{n\pi}{2}\right)E(t) \quad \text{with} \quad t = 1/\omega \tag{24}$$

Observe that it has been assumed n in (19) is essentially the same as n in (23). This assumption depends on n varying slowly with $\log t$ or $\log \omega$, and is confirmed by the examples given later.

Considering next the Carson transform in terms of E'', (13), it is seen that $(\tilde{E}-E_e)/s$ in terms of E''/ω is analogous to (12). Equation (A4) in Appendix A shows that E''/ω is a monotone, decreasing function of ω. However, the magnitude of the log–log slope approaches two at high frequencies [cf (A4)], which is far greater than that for E'; in fact, for a pure power law $(E''/\omega) \sim \omega^{-2}$, and the integral (13) does not converge. Moreover, as shown in Appendix B, the optimum point of evaluation for ω_n is not close to s at intermediate frequencies near the point where the slope of E'' vanishes.

Nevertheless, let us use (13) while recognizing the resulting approximations will be good over only a limited frequency range. Results like (23) and (24) are found, but with the changes $E' \to E''$, $\tilde{E} \to \tilde{E}-E_e$ and $\cos \to \sin$. By combining these results, we find

$$E''(\omega) = \tan\left(\frac{n\pi}{2}\right)[E'(\omega)-E_e] \tag{25}$$

where the local slope is now

$$n \equiv \frac{\mathrm{d}\log[E'(\omega)-E_e]}{\mathrm{d}\log\omega} \tag{26}$$

Clearly, when $n \geqslant 1$, this result is not valid. Note from (A3) that $n \to 2$ as $\omega \to 0$, showing that (25) will not be valid at very low frequencies.

As an alternative approach, we may use a modified form of (11),

$$E''(\omega) = \frac{2\omega}{\pi}\int_0^\infty E'(\lambda)\frac{1}{\lambda^2-\omega^2}\,\mathrm{d}\lambda \tag{27}$$

which also has a narrow band weight function. This form is obtained by recognizing that the part of the integral (11) involving E_e vanishes. As before, use (22) but neglect F'; then

$$E''(\omega) = \tan\left(\frac{n\pi}{2}\right)E'(\omega) \tag{28}$$

where now

$$n \equiv \frac{\mathrm{d}\log E'(\omega)}{\mathrm{d}\log\omega} \tag{29}$$

We may use the low frequency behavior of E' in (A3) to check the validity of (28) as $\omega \to 0$. It is found that the result is different from the limit derived using (A4), and thus neither (25) nor (28)

are valid for this case. Similarly, we find that (25) and (28) do not predict the correct limiting behavior for $\omega \to \infty$. However, simple, exact expressions may be derived from (11) for the low and high frequency limits. Specifically, we find

$$E''(\omega) \to c_1 \omega \quad \text{as } \omega \to 0 \tag{30}$$

and

$$E''(\omega) \to \frac{c_2}{\omega} \quad \text{as } \omega \to \infty \tag{31}$$

where

$$c_1 \equiv \frac{2}{\pi} \int_0^\infty [E'(\lambda) - E_e] \frac{d\lambda}{\lambda^2} \tag{32}$$

and

$$c_2 \equiv \frac{2}{\pi} \int_0^\infty [E_g - E'(\lambda)] \, d\lambda \tag{33}$$

where E_g is the glassy modulus. The result (33) was obtained from (11) by adding E_e–E_g to the integrand; this step of adding a constant has no effect on the integral, but is needed to achieve convergence when $\omega \to \infty$. Equations (31)–(33) may be used with experimental data to complete the prediction of E'' when combined with (25) or (28), as illustrated later. If the Prony series constants are available, (A4) may be used to obtain c_1 and c_2 more simply,

$$c_1 = \sum_{i=1}^{m} \rho_i E_i, \quad c_2 = \sum_{i=1}^{m} E_i / \rho_i \tag{34}$$

Simple asymptotic results for other functions could be easily derived for use when the approximate interrelationships breakdown, but the ones recorded here are the only ones needed in the subsequent discussion.

4. New approximate interconversion method

Equations (19), (23) and (28) may be combined and rearranged to summarize the set of approximate interconversions:

$$\tilde{E}(s) \cong \tilde{\lambda} E(t)|_{t=(1/s)} \quad \text{or} \quad E(t) \cong \frac{1}{\tilde{\lambda}} \tilde{E}(s)|_{s=(1/t)} \tag{35}$$

$$E'(\omega) \cong \lambda' E(t)|_{t=(1/\omega)} \quad \text{or} \quad E(t) \cong \frac{1}{\lambda'} E'(\omega)|_{\omega=(1/t)} \tag{36}$$

$$E''(\omega) \cong \lambda'' E(t)|_{t=(1/\omega)} \quad \text{or} \quad E(t) \cong \frac{1}{\lambda''} E''(\omega)|_{\omega=(1/t)} \tag{37}$$

$$E'(\omega) \cong \hat{\lambda}\tilde{E}(s)|_{s=\omega} \quad \text{or} \quad \tilde{E}(s) \cong \frac{1}{\hat{\lambda}} E'(\omega)|_{\omega=s} \tag{38}$$

$$E''(\omega) \cong \bar{\lambda}\tilde{E}(s)|_{s=\omega} \quad \text{or} \quad \tilde{E}(s) \cong \frac{1}{\bar{\lambda}} E''(\omega)|_{\omega=s} \tag{39}$$

$$E''(\omega) \cong \lambda^* E'(\hat{\omega})|_{\hat{\omega}=\omega} \quad \text{or} \quad E'(w) \cong \frac{1}{\lambda^*} E''(\hat{\omega})|_{\hat{\omega}=\omega} \tag{40}$$

where the adjustment factors, $\tilde{\lambda}$, λ', λ'', $\hat{\lambda}$, $\bar{\lambda}$ and λ^* are given in Table 1 as functions of n. Relations (35)–(40) are exact when the material functions are described by pure power laws; however, these are shown as approximate relationships allowing for behavior which does not exactly obey a power law over $0 < t, s, \omega < \infty$. One should interpret n as the local, log–log slope of the source function at the specified position. For instance, for the case of (35), $n = -\mathrm{d}\log E(t)/\mathrm{d}\log t$ at $t = 1/s$ when $E(t)$ is the source function, and $n = \mathrm{d}\log \tilde{E}(s)/\mathrm{d}\log s$ at $s = 1/t$ when $\tilde{E}(s)$ is the source function.

It should be stressed that the equations with E'' as the source function have a limited range of validity, but are given here for completeness. Also, we have assumed that the n-value may be taken as the log–log slope of the source function, regardless of which function was used in the original development of the equation; e.g., $E(t)$ is the source function in (19), but $\tilde{E}(s)$ is the source function in the second part of (35). This procedure is valid for a slowly varying slope.

Consider now a power-law creep compliance,

$$D(t) = D_1 t^n \tag{41}$$

Relations similar to (15)–(40) hold for compliance functions when appropriate changes of parameters are made; i.e., $E_1 \to D_1$, $n \to -n$, $\tilde{E} \to \tilde{D}$, $E' \to D'$, and $E'' \to -D''$. It should be noted that the sign change in $E'' \leftrightarrow -D''$ requires that the sign of n be used because the argument of the trigonometric functions that appear in the λ-function definitions should not change when modulus and compliance are interchanged.

The adjustment functions, λ's, defined in Table 1, are plotted in Fig. 2(a) and 2(b) for $-1 < n < 1$. The λ-curves in Fig. 2(a) are not symmetric about the $n = 0$ axis because of the change in sign of n in the gamma function; thus, the first three λ's in Table 1 required for a

Table 1
Adjustment functions used in new approximate interconversion method

Ratios	Adjustment functions
$\tilde{\lambda} = \tilde{E}(s)/E(t)$	$\tilde{\lambda} = \Gamma(1-n)$
$\lambda' = E'(\omega)/E(t)$	$\lambda' = \Gamma(1-n)\cos(n\pi/2)$
$\lambda'' = E''(\omega)/E(t)$	$\lambda'' = \Gamma(1-n)\sin(n\pi/2)$
$\hat{\lambda} = E'(\omega)/\tilde{E}(s)$	$\hat{\lambda} = \cos(n\pi/2)$
$\bar{\lambda} = E''(\omega)/\tilde{E}(s)$	$\bar{\lambda} = \sin(n\pi/2)$
$\lambda^* = E''(\omega)/E'(\omega)$	$\lambda^* = \tan(n\pi/2)$

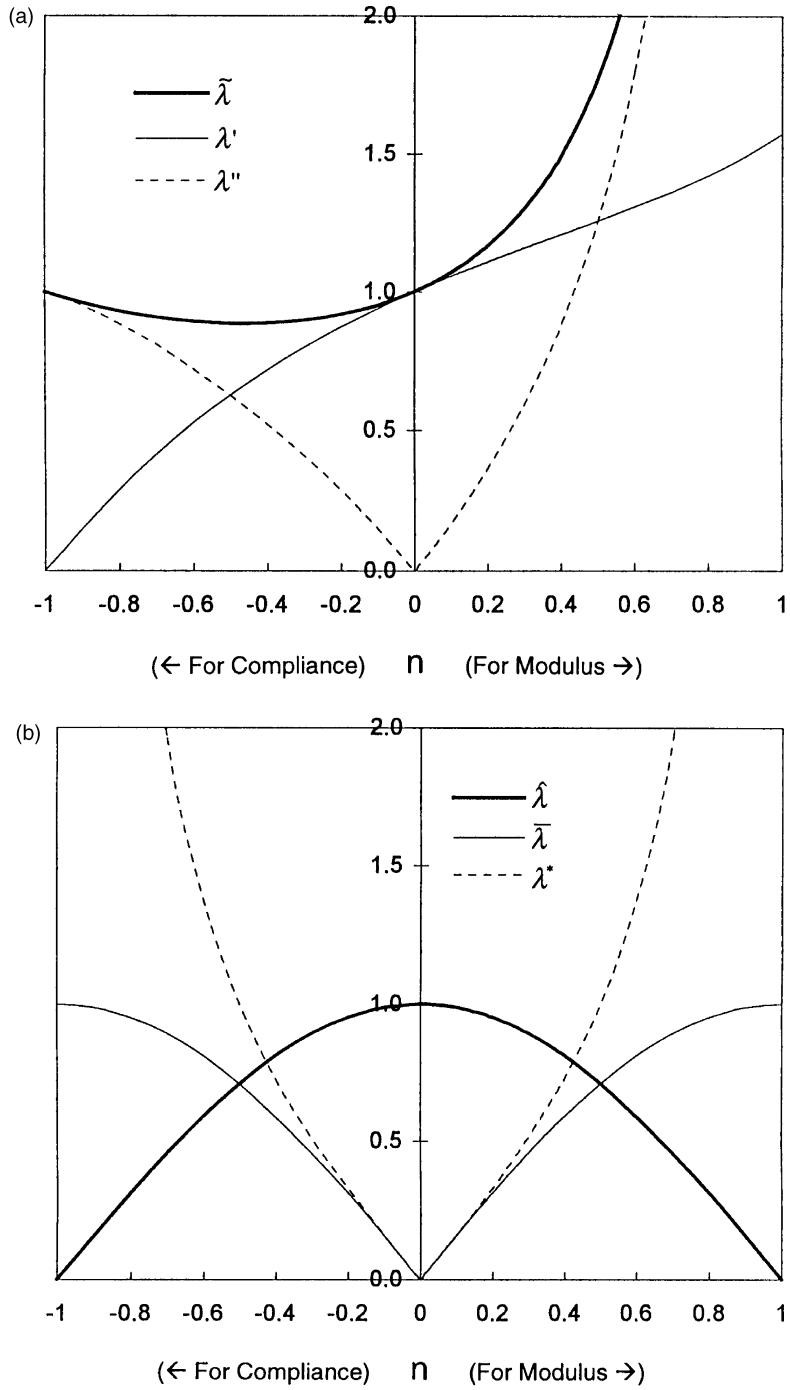

Fig. 2. Graphical representation of adjustment functions. (a) $\tilde{\lambda}(n)$, $\lambda'(n)$ and $\lambda''(n)$. (b) $\hat{\lambda}(n)$, $\bar{\lambda}(n)$ and $\lambda^*(n)$.

compliance interconversion differs from that required for the corresponding modulus interconversion for the same (absolute) value of n.

It is of interest to apply (35) to both the modulus and compliance functions and use the exact relationship, $\tilde{E}(s)\tilde{D}(s) = 1$. Assuming, as before, a local power law behavior, this process yields Ferry's (1970) equation,

$$E(t)D(t) = \Gamma(1-n)\Gamma(1+n) = \frac{\sin n\pi}{n\pi} \tag{42}$$

where n is again the local log–log slope. This equation has been found to be very accurate for broadband functions, as reported by Ferry (1970) and as we have found in our unpublished studies; the theory in the previous section shows why it works so well.

Finally, for viscoelastic solids we note that the nonzero equilibrium modulus E_e must be explicitly added to the far right-hand sides of (37), (39) and (40) to obtain good results as $t \to \infty$ and $s, \omega \to 0$ if E'' is the source function. This is certainly clear because E'' is independent of E_e. More generally, the exact interrelationships (9), (10), and (13) show that E_e is to be added to the integrals containing E''. Figure 3 demonstrates that the behavior of $E' - E_e$ is much closer to E'' than E' is at low frequencies. Similar behavior exists when E' is replaced by E or $\tilde{E}$. Consequently, in lieu of (37), (39) and (40), the following improved interconversions may be used for viscoelastic solids:

$$E''(\omega) \cong \lambda''[E(t) - E_e]|_{t=(1/\omega)} \quad \text{or} \quad E(t) \cong E_e + \frac{1}{\lambda''}E''(\omega)|_{\omega=(1/t)} \tag{43}$$

$$E''(\omega) \cong \tilde{\lambda}[\tilde{E}(s) - E_e]|_{s=\omega} \quad \text{or} \quad \tilde{E}(s) \cong E_e + \frac{1}{\tilde{\lambda}}E''(\omega)|_{\omega=s} \tag{44}$$

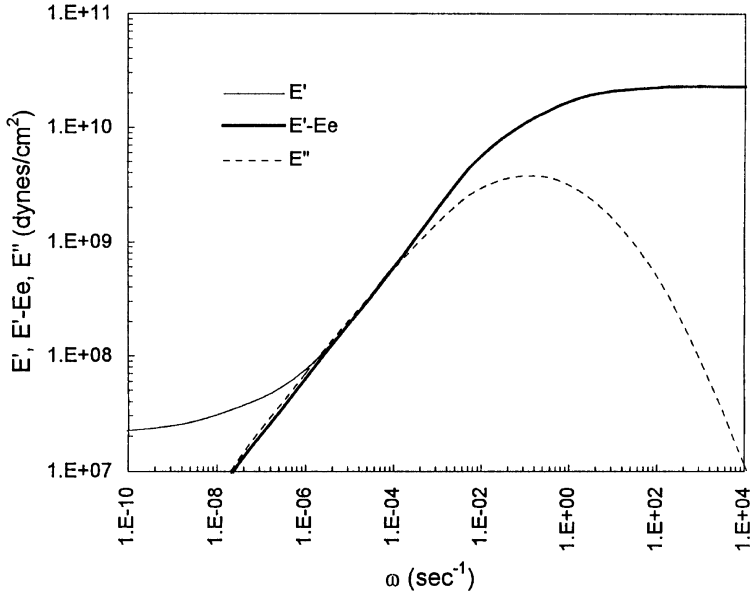

Fig. 3. Comparison of behavior of $E'(\omega)$, $E'(\omega) - E_e$ and $E''(\omega)$ for PMMA.

$$E''(\omega) \cong \lambda^*[E'(\hat{\omega}) - E_e]|_{\hat{\omega}=\omega} \quad \text{or} \quad E'(\omega) \cong E_e + \frac{1}{\lambda^*} E''(\hat{\omega})|_{\hat{\omega}=\omega} \tag{45}$$

where the adjustment factors λ'', $\bar{\lambda}$ and λ^* are as defined above as functions of n; however, the log–log slope n in these cases is defined as $\mathrm{d}\log E''/\mathrm{d}\log\omega$ when E'' is the source function, or as $-\mathrm{d}\log(E-E_e)/\log, t$, $\mathrm{d}\log(\tilde{E}-E_e)/\log s$ or $\mathrm{d}\log(E'-E_e)/\log\omega$ when E, $\tilde{E}$ or E' are the source functions, respectively. Equations (43)–(45) are easily shown to be exact when n is constant.

As mentioned above, the modified eqns (43)–(45) must be used to obtain E, $\tilde{E}$ or E' from E'' when $t \to \infty$ or $s, \omega \to 0$. However, when E'' is to be predicted, the modified equations are found, by a study of examples, to offer only a small improvement over (37), (39) and (40).

5. Numerical examples

We shall now illustrate the approximate interconversion method described above for PMMA material functions. The constants in the Prony series representation (A1) of the relaxation modulus of PMMA provide what we call exact representations of the material functions in (A1)–(A4). These constants are the same as used in the companion paper (Park and Schapery, 1998). Of course, it is not implied that these are exact representations of experimental data; however, for a given set of constants, they are exact and thus provide a means for checking the accuracy of the approximate interrelationships in this paper.

First, let us consider conversions of $\tilde{E}(s)$, $E'(\omega)$ and $E''(\omega)$ into $E(t)$; the first three functions come from (A2)–(A4). All the methods discussed above were tested and the results are plotted in Fig. 4(a). Many of the results are so close to each other that they are not easily distinguishable graphically. For an effective comparison of the accuracy of each method, the logarithmic deviation of each curve from the exact one, $\log(E/E_{\text{exact}})$, is plotted in Fig. 4(b).

It is seen that the methods employed produce good results in most cases. The conversion from E'' by means of (43) is good up to the value of $t = 1/\omega$ where the log–log slope of E'' begins to decrease noticeably with increasing ω (cf Fig. 3). For negative n values, the parameter λ'' is negative, which is physically unrealistic; thus, (43) fails as this unrealistic limit is approached. Recall that the n-values used here are all obtained from the log–log slope of the source function evaluated at $s = 1/t$ or $\omega = 1/t$.

Additional improvement in accuracy is achieved when optimum values of n, evaluated at $s = a/t$ or $\omega = b/t$ where a and b are functions of n as discussed in Appendix B, are employed. Maximum improvement is observed in the regions of highest curvature. For example, the maximum error of 8.6% ($\log E/E_{\text{exact}} = 0.036$) in the $\tilde{E}(s) \to E(t)$ conversion at around $t = 1\text{E}+06$ s [Fig. 4, predicted by eqn (35)] reduces to 4.1% ($\log E/E_{\text{exact}} = 0.017$) when the n value is evaluated from $\tilde{E}(s)$ at $s = 0.316/t$. It is to be noted that this additional accuracy is obtained at the expense of an extra effort of locating the optimum n-value evaluation positions.

Conversions of $\tilde{D}(s)$, $D'(\omega)$ and $D''(\omega)$ to $D(t)$ for PMMA were also carried out in a similar manner. Even though the results are not included in this paper because of space limitation, similar findings were observed. It is to be recalled, however, that the λ-functions as shown in Fig. 2 are not symmetric about the $n = 0$ axis and therefore the performance of each equation discussed above is slightly different when applied to compliance functions compared to modulus functions.

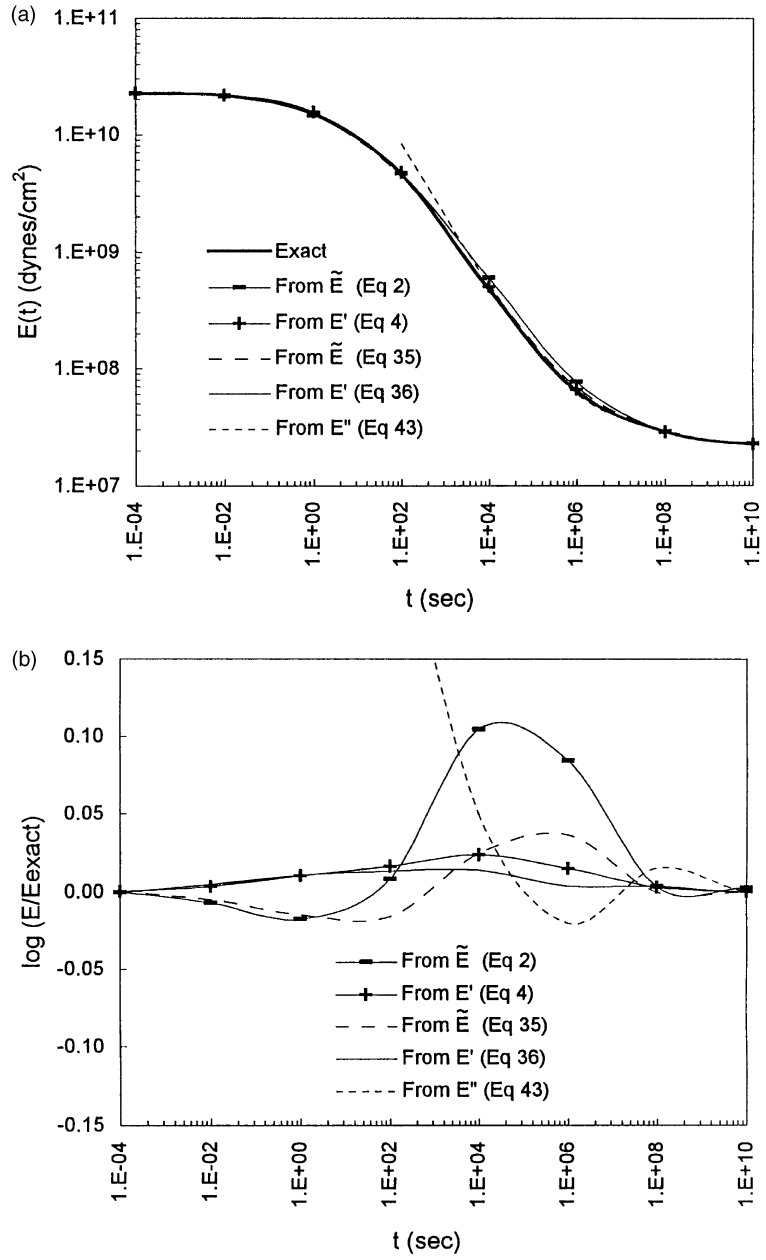

Fig. 4. The relaxation modulus $E(t)$ converted from $\tilde{E}(s)$, $E'(\omega)$ and $E''(\omega)$. (a) Graphical representation on log–log scales. (b) Logarithmic deviations from the exact solution.

For a similar reason, it was observed that (2) works better than (4) in a compliance interconversion, while the opposite is true in a modulus interconversion.

Next, conversions from E, E' and E'' to $\tilde{E}$ were tested; like before, the first three come from

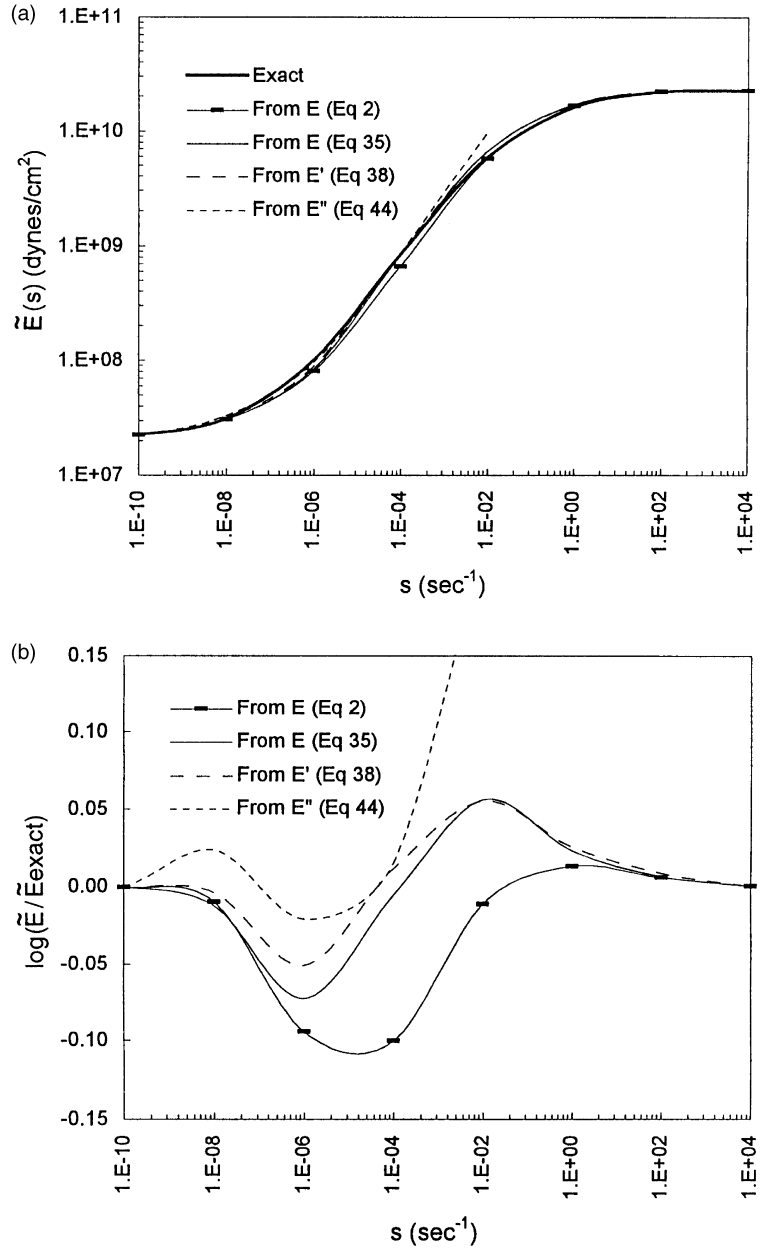

Fig. 5. The operational modulus $\tilde{E}(s)$ converted from $E(t)$, $E'(\omega)$ and $E''(\omega)$. (a) Graphical representation on log–log scales. (b) Logarithmic deviations from the exact solution.

(A1), (A2) and (A4). The results are shown in Fig. 5(a) and (b). Again, Fig. 5(b) is provided to show the differences among the methods more effectively. Overall, the degree of accuracy and the characteristics of performance are about the same as for the previous case. All the new proposed

equations work well. Again, the conversion of E'' to $\tilde{E}$ worked only up to where the log–log slope of E'' begins to decrease noticeably with increasing frequency.

Conversions from E, $\tilde{E}$ and E'' to E' were also conducted and the results are presented in Fig. 6(a) and (b). Similar performance is observed as in the two preceding cases. The method proposed by Booij and Thoone (1982) using (7) was also considered; it shows a trend similar to that of (45), even though its accuracy is less at intermediate frequencies.

Finally, conversions from E, $\tilde{E}$ and E' to E'' were carried out and the results are shown in Fig. 7(a) and (b). Also shown are the asymptotic predictions using (30) and (31). The new method yields good results within the mid-range of the frequency. In the low and high frequency regions (corresponding to the rubbery and glassy plateau zones), the accuracy decreases; the behaviors of adjustment functions λ'', $\bar{\lambda}$ and λ^* shown in Fig. 2 indicate that as n grows or approaches zero these functions correspondingly grow rapidly (except $\bar{\lambda}$) or approach zero thus resulting in poor predictions. Conversions for $\omega < 1.E\text{-}8$ were not used because n's approached or exceeded unity. However, the difficulties in the low and high frequency regions can be mitigated by using the asymptotic formulas (30) and (31). It is seen that fairly good predictions can be obtained over the entire frequency range, $0 < \omega < \infty$, by blending the approximate predictions into the exact asymptotic lines.

The existing conversion from E' to E'' in (5), proposed by Staverman and Schwarzl (1955) was also employed and turned out to produce results comparable to those by the new method, as given by (45). It is noteworthy that (5) and (7) can be rewritten, respectively, in terms of the log–log slope n,

$$E''(\omega) \cong \frac{n\pi}{2}[E'(\hat{\omega}) - E_e]|_{\hat{\omega}=\omega} \tag{46}$$

$$E'(\omega) \cong E_e + \frac{(1-n)\pi}{2} E''(\hat{\omega})|_{\hat{\omega}=\omega} \tag{47}$$

where $n \equiv \mathrm{d}\log(E' - E_e)/\mathrm{d}\log\omega = \mathrm{d}\ln(E' - E_e)/\mathrm{d}\ln\omega$ or $n \equiv \mathrm{d}\log E''/\mathrm{d}\log\omega$, depending on the source function. The constant E_e (equilibrium modulus) has been included in (46) as a free integration constant so that (46) can be directly compared with (45). It is seen that λ^* and $1/\lambda^*$ correspond, respectively, to the simple linear functions $n\pi/2$ and $(1-n)\pi/2$; their overall behavior agree qualitatively. When E'' obeys a pure power law, the relations in (45) are exact, regardless of n, while (46) and (47) are not exact. It should be mentioned that $0 \leqslant n < 0.4$ for all PMMA functions, except for E''. Thus, replacement of $\tan(n\pi/2)$ by $(n\pi/2)$, as implied by (46), is only a crude approximation in the frequency range for which n is not small.

6. Further discussion

Through the preceding examples for PMMA, we have seen that the new interconversion method improves results over the existing methods without adding any procedural complexity. However, in order to check the validity and accuracy of the method for uncommon cases of narrow-band material functions, two additional tests have been conducted.

As the first case, an artificial relaxation modulus $E(t)$ simulating that of the foregoing PMMA,

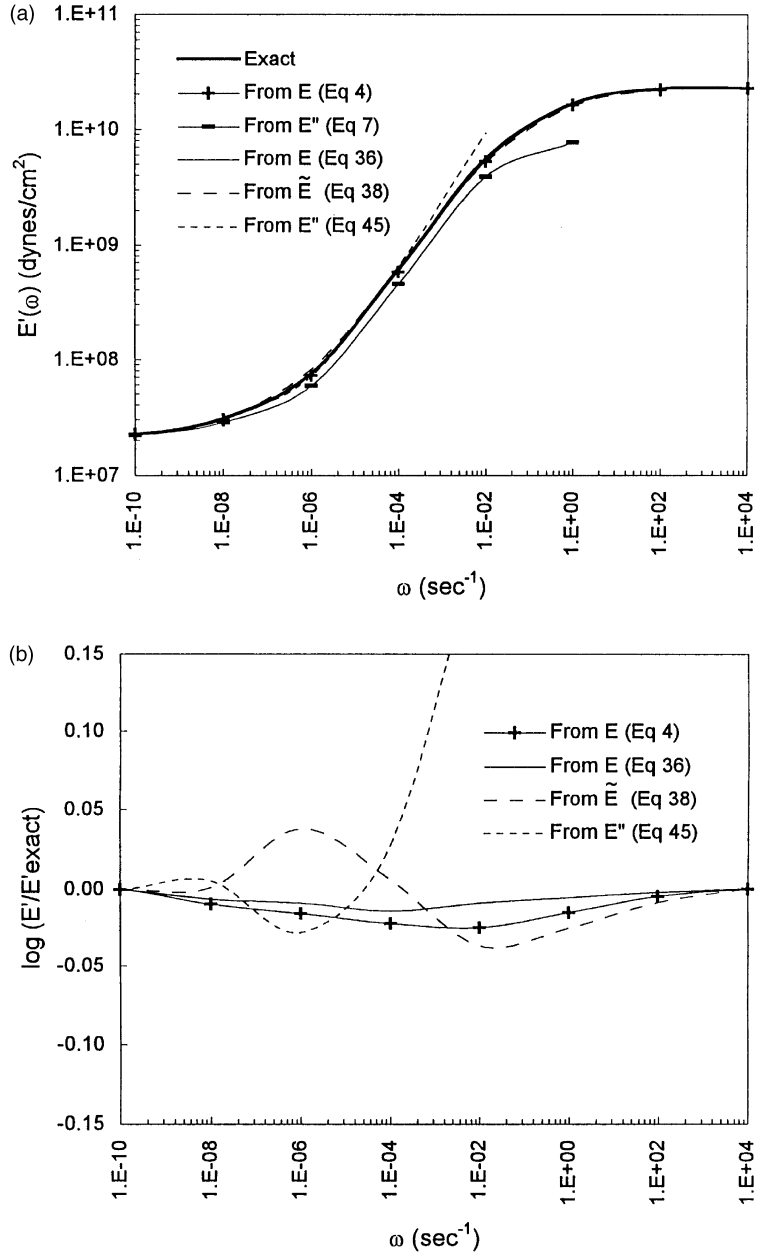

Fig. 6. The storage modulus $E'(\omega)$ converted from $E(t)$, $\tilde{E}(s)$ and $E''(\omega)$. (a) Graphical representation on log–log scales. (b) Logarithmic deviations from the exact solution.

but using a 5-term ($m = 5$) Prony series representation (with relaxation times, $\rho_i = 10^{(i-1)}$; $i = 1, \ldots, 5$), was considered (Fig. 8). Our original $E(t)$ for PMMA was represented by an 11-term Prony series in our companion paper (Park and Schapery, 1998). A comparison of Figs 4(a) and

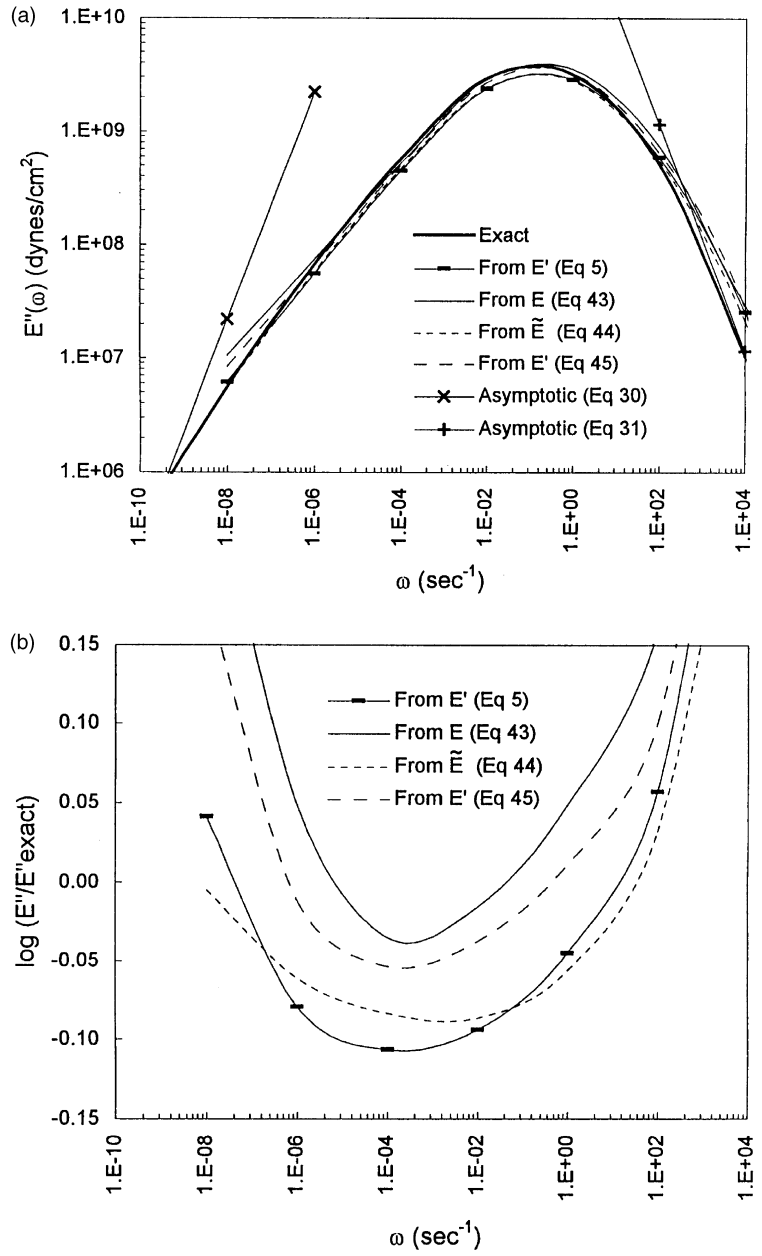

Fig. 7. The loss modulus $E''(\omega)$ converted from $E(t)$, $\tilde{E}(s)$ and $E'(\omega)$. (a) Graphical representation on log–log scales. (b) Logarithmic deviations from the exact solution.

8 indicates that the glassy and the equilibrium moduli were left unchanged but, as shown in Figs 4(a) and 8, the slope of the curves in the transition zone are quite different and the curvature near the toe of the $m = 5$ curve is larger than that for $m = 11$. Equations (35) for $\tilde{E}$ and (36) for E'

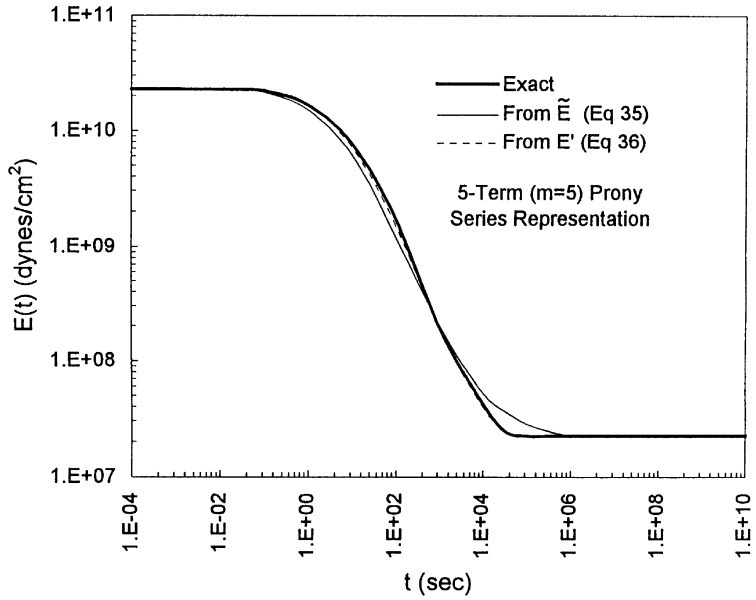

Fig. 8. The relaxation modulus $E(t)$ converted from $\tilde{E}(s)$ and $E'(\omega)$ when the source functions are represented by a 5-term Prony series.

were applied using the new exact representations of $\tilde{E}$ and E'. The result from (35) shows some deviations from the new exact $E(t)$ in (A1) with $m = 5$, especially around the toe zone, but (36) still gives a good prediction of $E(t)$. The difference between E' and $\tilde{E}$ becomes more pronounced as the number of Prony series terms decreases in the representation of $E(t)$.

As the second case, an extreme case of one-term ($N = 1$) Prony series representation was considered, again maintaining the same glassy and the equilibrium moduli of the PMMA (Fig. 9). The slope of the curve within the transition zone and the curvature at the toe are extremely high. It turned out that (36) fails over part of the time range in this case because of the excessive log–log slope of the source curve ($n > 1$). Method (35) was found to be qualitatively good because the log–log slope of the source functions stays within the allowable range ($0 \leqslant n < 1$); however, the accuracy was not good.

With these additional examples, we have shown that the proposed method leads to poor results when the source and target functions exhibit large curvature on log–log coordinates. This is not surprising since, in this case, n is not a slowly varying function of logarithmic values of t, ω or s.

7. Conclusions

A new analytical method of approximate interconversion of linear viscoelastic material functions and approximate Laplace transformation and inversion (for these and other functions) was introduced and its performance checked successfully using viscoelastic functions for PMMA. The method employs variable adjustment factors (or vertical shift factors on a logarithmic scale) dictated by the slope of the source function on a doubly-logarithmic scale.

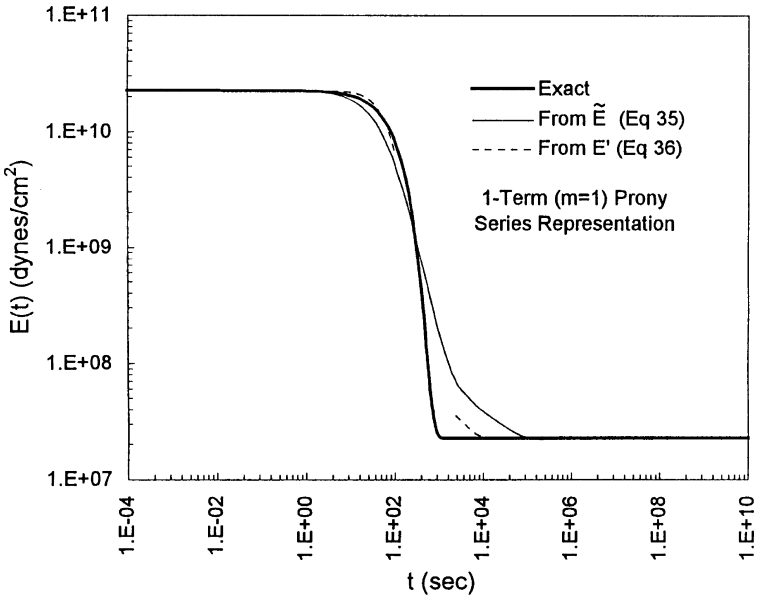

Fig. 9. The relaxation modulus $E(t)$ converted from $\tilde{E}(s)$ and $E'(\omega)$ when the source functions are represented by a 1-term Prony series.

Some available existing methods were reviewed and their performance compared with that of the new method. The existing methods exhibited varying degrees of success, but the new method has been shown to yield improved results over the existing methods. The theoretical basis, in terms of the mathematical properties of the weight functions involved in the exact interrelationships, was discussed and explains the improvement that has been observed in the new method.

Even though the method is illustrated in this paper through the interconversion of modulus functions, the method is equally applicable to the interconversion of compliance functions. It has the same theoretical basis as that for the modulus functions.

Appendix A: representation of modulus functions based on the Prony series

Relaxation modulus (Prony series):

$$E(t) = E_e + \sum_{i=1}^{m} E_i e^{-t/\rho_i} \tag{A1}$$

Operational modulus:

$$\tilde{E}(s) = E_e + \sum_{i=1}^{m} \frac{s\rho_i E_i}{s\rho_i + 1} \tag{A2}$$

Storage modulus:

$$E'(\omega) = E_e + \sum_{i=1}^{m} \frac{\omega^2 \rho_i^2 E_i}{\omega^2 \rho_i^2 + 1} \tag{A3}$$

Loss modulus:

$$E''(\omega) = \sum_{i=1}^{m} \frac{\omega \rho_i E_i}{\omega^2 \rho_i^2 + 1} \tag{A4}$$

where E_e, E_i and ρ_i are constants. According to linear thermodynamics for stable systems obeying Onsager's principle (Biot, 1954), all linear viscoelastic materials can be described with these forms and all of the constants are positive when the modulus is the ratio of stress to its work-conjugate strain. When considering the general case of the modulus tensor for isotropic and anisotropic media, each coefficient in (A1) is replaced by a positive–definite matrix.

Appendix B: determination of optimum location for slope evaluation

The approximate method described in the body of this paper uses the local log–log slope of the relevant material functions. Referring to (1), (12) and (13), the problem posed here is to determine the time or frequency at which the slope should be evaluated to minimize the error in evaluating each integral.

Let us consider first the operational modulus, or the Carson transform of the relaxation modulus, (1). For a given value of s, the optimum location depends on how the relaxation modulus varies relative to a pure power law. Specifically, suppose for a given s that over the range for which the weight function is not essentially zero we use a special case of (15),

$$E(t) = E_n \left(\frac{t}{t_n}\right)^{-n} \left[1 + k\left\{\log\left(\frac{t}{t_n}\right)\right\}^2\right] \tag{B1}$$

where k is a constant for a given t_n. Then,

$$\log E(t) = \log E_n - n \log\left(\frac{t}{t_n}\right) + \log\left[1 + k\left\{\log\left(\frac{t}{t_n}\right)\right\}^2\right] \tag{B2}$$

If, over the band width of the weight function, the departure from a power law is small, then the last term in (B2) is approximately $k(\log t - \log t_n)^2$. The difference between a tangent line at t_n and the actual function $\log E$ is thus a quadratic in $\log t$, implying constant curvature in logarithmic coordinates. More generally, except at an inflection point (where the error is certainly small), (B1) provides a simple, apparently realistic correction to a power law over the significant band width of the weight function.

With F from (B1), the correction c_n in (18) is minimized with respect to t_n to find

$$\int_0^\infty e^{-st} t^{-n} (\log t - \log t_n)\, dt = 0 \tag{B3}$$

so that

$$\log t_n = \int_0^\infty e^{-st} t^{-n} \log t \, \mathrm{d}t \Big/ \int_0^\infty e^{-st} t^{-n} \, \mathrm{d}t \tag{B4}$$

[The assumed weak dependence of n on t_n has been neglected in arriving at (B3).] When (B4) is expressed in terms of $\log t$ as the integration variable, it may be seen that $\log t_n$ is placed at the centroid of the function $e^{-st}t^{1-n}$. For $0 < n < 1$, this location is to the left of the centroid of $g(w)$ in Fig. 1 (which is for the function $e^{-st}t$). Equation (B4) simplifies to

$$\log(st_n) = I_1 \frac{\log e}{\Gamma(1-n)} \tag{B5}$$

where I_1 is the integral

$$I_1 \equiv \int_0^\infty e^{-u} u^{-n} \ln u \, \mathrm{d}u \tag{B6}$$

which may be evaluated analytically (Gradshteyn and Ryzhik, 1965). For a few values of n we find

$$\begin{aligned} &n = 0, \quad \log(st_n) \cong -0.25 \\ &n = 0.25, \quad \log(st_n) \cong -0.47 \\ &n = 0.5, \quad \log(st_n) \cong -0.85 \\ &n = 0.75, \quad \log(st_n) \cong -1.82 \end{aligned} \tag{B7}$$

Since n is not initially given, an iteration procedure is needed if the resulting slope is not close to the original estimate. The departure from a power law is usually greatest when n is much smaller than 0.5 (at short and long times), and therefore the optimum value of $\log(st_n)$ is small in the regions of high curvature. For example, if $n = 0.25$ then the optimum location is less than one-half decade to the left of what was used in the body of the paper, $\log(st_n) = 0$. When $n < 0$ (for creep compliance), the optimum (centroid) location is even closer to the $\log(st_n) = 0$; for the extreme case of $n = -1$, we find $\log(st_n) \cong 0.18$.

A similar approach may be used in evaluating $\tilde{E}$ from E' and E''. Specifically, use a form of E' like that for E in (B1), but with t/t_n replaced by ω/ω_n and $-n$ by n. The optimum location is given by,

$$\log(\omega_n/s) = \int_0^\infty \frac{z^n \log z \, \mathrm{d}z}{1+z^2} \Big/ \int_0^\infty \frac{z^n \, \mathrm{d}z}{1+z^2} \tag{B8}$$

The integrals converge for $-1 < n < 1$, and may be analytically integrated to find

$$\log(\omega_n/s) = \frac{\pi}{2}(\log e) \tan\frac{n\pi}{2} \simeq 0.682 \tan\frac{n\pi}{2} \tag{B9}$$

For example,

$$n = 0, \quad \log(\omega_n/s) = 0$$
$$n = 0.25, \quad \log(\omega_n/s) \cong 0.28$$
$$n = 0.5, \quad \log(\omega_n/s) \cong 0.68$$
$$n = 0.75, \quad \log(\omega_n/s) \cong 1.65 \tag{B10}$$

It is seen that the values are somewhat smaller in magnitude than those in (B7) for the relaxation modulus. Thus, the optimum slope evaluation point is at or to the right of the point used in the body of the paper, $\log(\omega_n/s) = 0$.

For E'', we represent E''/ω in the form of (B1) but with t/t_n replaced by ω/ω_n and n by q,

$$q \equiv -\frac{\mathrm{d}\log(E''/\omega)}{\mathrm{d}\log\omega} = 1 - \frac{\mathrm{d}\log E''}{\mathrm{d}\log\omega} \tag{B11}$$

which is always non-negative. Then, use (B9) after replacing n by $-q$. Thus,

$$\log(\omega_n/s) \cong -0.682\tan\frac{q\pi}{2} \tag{B12}$$

In this case, $\log(\omega_n/s) < 0$ and it is unbounded at an intermediate frequency where E'' exhibits a maximum with respect to frequency.

Acknowledgement

Sponsorship of the contribution of the first author by the Office of Naval Research, Ship Structures and System, S&T Division, and the National Science Foundation through the Offshore Technology Research Center, is gratefully acknowledged.

References

Biot, M.A., 1954. Theory of stress–strain relations in anisotropic viscoelasticity and relaxation phenomena. Journal of Applied Physics 25, 1385–1391.

Booij, H.C., Thoone, G.P.J.M., 1982. Generalization of Kramers–Kronig transforms and some approximations of relations between viscoelastic quantities. Rheologica Acta 21, 15–24.

Christensen, R.M., 1982. Theory of Viscoelasticity. 2nd edn. Academic Press, New York.

Cost, T.L., Becker, E.B., 1970. A multidata method of approximate Laplace transform inversion. International Numerical Methods in Engineering 2, 207–219.

Ferry, J.D., 1970. Viscoelastic Properties of Polymers, 2nd edn. John Wiley and Sons, New York.

Ferry, J.D., 1980. Viscoelastic Properties of Polymers, 3rd edn. John Wiley and Sons, New York.

Gradshteyn, I.S., Ryzhik, I.M., 1965. Tables of Integrals, Series, and Products. Academic Press, New York.

Park, S.W., Schapery, R.A., 1998. Methods of interconversion between linear viscoelastic material functions. Part I—a numerical method based on Prony series. International Journal of Solids and Structures 36, 1653–1675.

Schapery, R.A., 1961. A simple collocation method for fitting viscoelastic models to experimental data. GALCIT SM 61-23A, California Institute of Technology, Pasadena, CA.

Schapery, R.A., 1962. Approximate methods of transform inversion for viscoelastic stress analysis. Proc. 4th U.S. Nat. Cong. Appl. Mech. 1075–1085.

Schapery, R.A., 1974. Viscoelastic behavior and analysis of composite materials, Composite Materials, ed. G. P. Sendeckyj, Chap. 4, Vol. 2. pp. 85–168. Academic Press, New York.

Schwarzl, F.R., Struik, L.C.E., 1967. Analysis of relaxation measurements. Advances in Molecular Relaxation Processes 1, 201–255.

Staverman, A.J., Schwarzl, F., 1955. Physik der Hochpolymeren, ed. H. A. Stuart, pp. 1–121. Band IV. Springer-Verlag, Berlin.

Tschoegl, N.W., 1989. The Phenomological Theory of Linear Viscoelastic Behavior. Springer-Verlag, Berlin.